Zuerst erschienen in: Nuclear Engineering and Design 206 (2001), Seite 235–247
http://dx.doi.org/10.1016/S0029-5493(00)00438-6

Cyclic plastic deformation tests to verify FEM-based shakedown analyses

H. Lang [a,*], K. Wirtz [a], M. Heitzer [b], M. Staat [c], R. Oettel [d]

[a] *Siemens AG-Power Generation Group, Erlangen, Germany*
[b] *Jülich Research Center, Jülich, Germany*
[c] *Aachen University of Applied Science Div. Jülich, Jülich, Germany*
[d] *Siempelkamp Prüf-und Gutachtergesellschaft, Dresden, Germany*

Abstract

Fatigue analyses are conducted with the aim of verifying that thermal ratcheting is limited. To this end it is important to make a clear distintion between the shakedown range and the ratcheting range (continuing deformation). As part of an EU-supported research project, experiments were carried out using a 4-bar model. The experiment comprised a water-cooled internal tube, and three insulated heatable outer test bars. The system was subjected to alternating axial forces, superimposed with alternating temperatures at the outer bars. The test parameters were partly selected on the basis of previous shakedown analyses. During the test, temperatures and strains were measured as a function of time. The loads and the resulting stresses were confirmed on an ongoing basis during performance of the test, and after it. Different material models were applied for this incremental elasto-plastic analysis using the ANSYS program. The results of the simulation are used to verify the FEM-based shakedown analysis.

1. Introduction

Fatigue analyses are conducted with the aim of verifying that thermal ratcheting is limited in the event of the 3Sm criterion being exceeded. Various codes and standards (for example, KTA 3201.2, 6/96) use the Bree interaction diagram (Ng and Moreton, 1982) for this. In this approach, the allowable stress range induced by thermal loading as a function of primary stress is limited such that elastic shakedown is ensured. In the event of the allowable thermal stress range being exceeded, the accumulated plastic strain has to be limited.

With these approximation methods, plastic influences are largely taken into account through an elastic stress analysis with extrapolation of analytical results according to collapse load/shakedown theory, and the strain occurring is estimated on the basis of simple assumptions.

Incremental elasto-plastic analyses provide more realistic and accurate results. However, they necessitate greater calculation effort, and require detailed knowledge of load history and material law, neither of which can be guaranteed to be available to the requisite extent in practice.

* Corresponding author. Tel.: +49-9131-1899336; fax: +49-9131-1895007.

As part of an EU-supported research project (Staat and Heitzer, 1999), a technique was applied which calculates the collapse and shakedown load of ductile structures directly on the basis of FEM discretization, without stress analysis. This paper describes a test carried out using this technique, and draws a comparison with the results of the shakedown analysis and the incremental elasto-plastic analysis. Different material models were used as a basis for the latter.

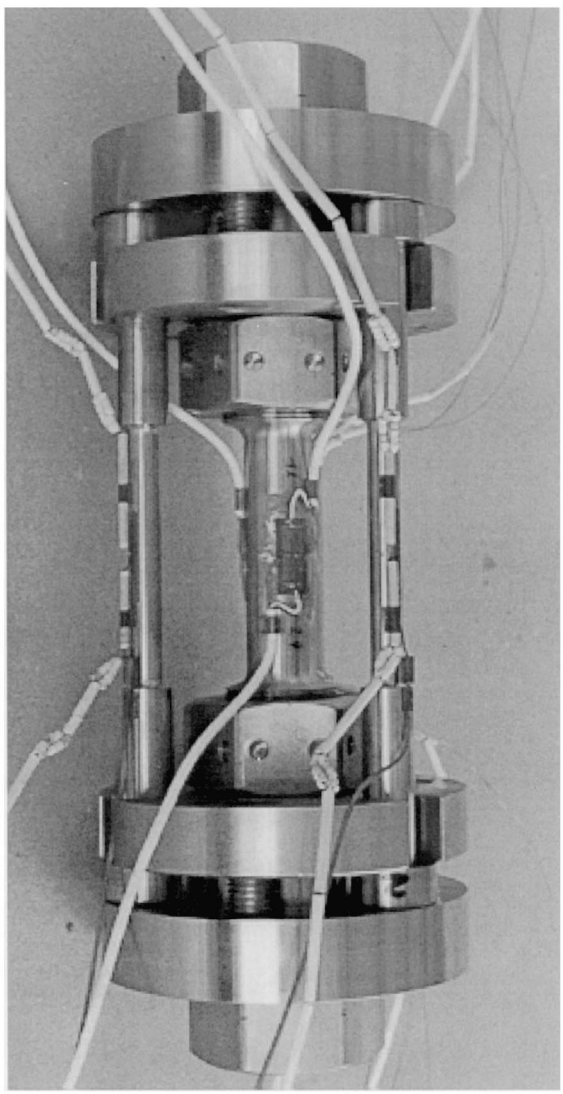

Fig. 1. Test specimen.

To date there is a shortage of tests involving cyclic, mechanical and thermal loads at the limit between shakedown and ratcheting. Two-bar experiments using copper at ambient temperature are described in Ponter (1983), in which the thermal strains are simulated by means of an electrical signal. Two-bar and multi-bar tests, enable representation of simple mechanical models of pipes and vessels subjected to internal pressure and a temperature gradient across the wall thickness. The tests presented here are aimed at determining a shakedown limit, below which failure due to ratcheting does not have to be assumed.

2. Test specimen

2.1. Geometry and material

The test specimen is shown in Fig. 1, and comprises the following components:

- cooled internal tube;
- internal nut;
- inner flange;
- three replaceable outer test bars;
- outer flange;
- three cap bolts, which brace the head of the test bars between the inner and outer flanges;
- external nut.

The test specimen is made from the austenitic steel 1.4550 (X6 CrNiNb 18 10).

2.2. Measuring points and measuring variables

Measurements were made at the following points (see Fig. 2, bottom):

	Measuring point
Temperature measurements	Hot test bar
	Cold internal tube
	Inner flange
	Cooling water outlet
Strain measurements	Hot test bar
	Cold internal tube

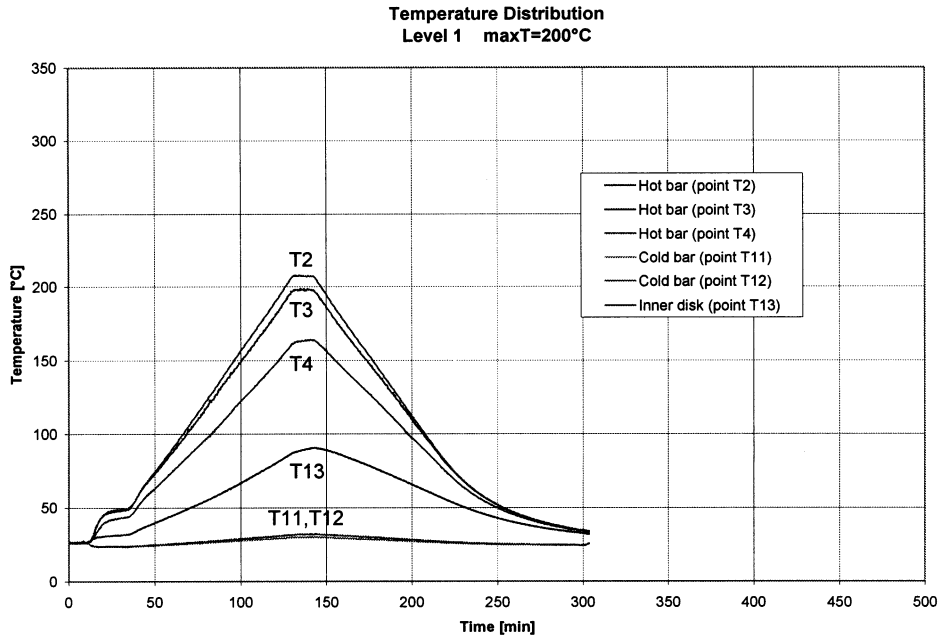

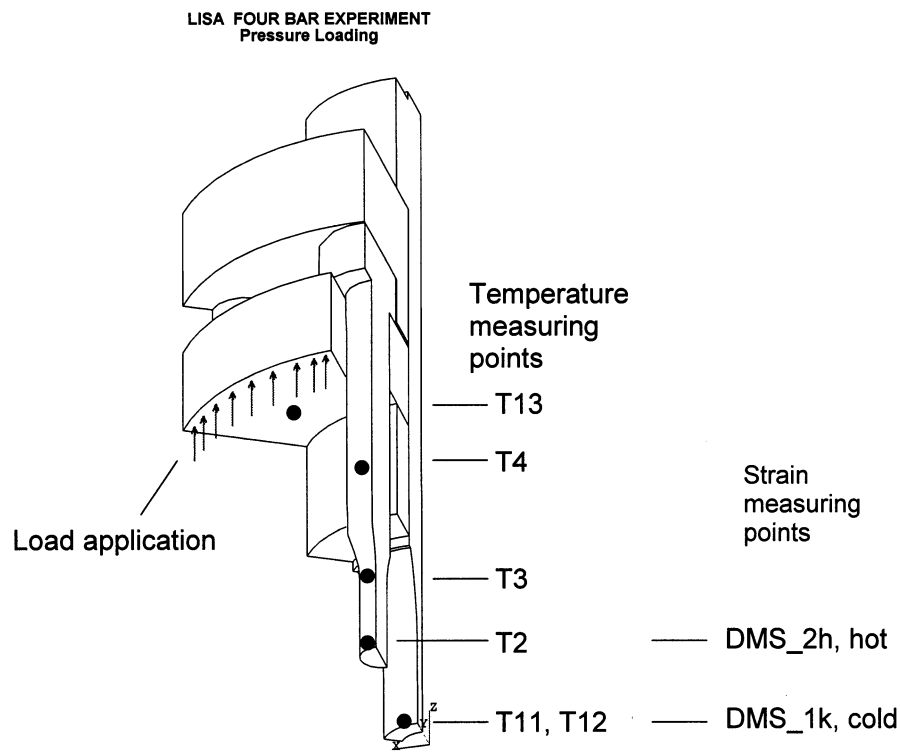

Fig. 2. Temperatures at load step 1; measuring points and load application (1/12 section).

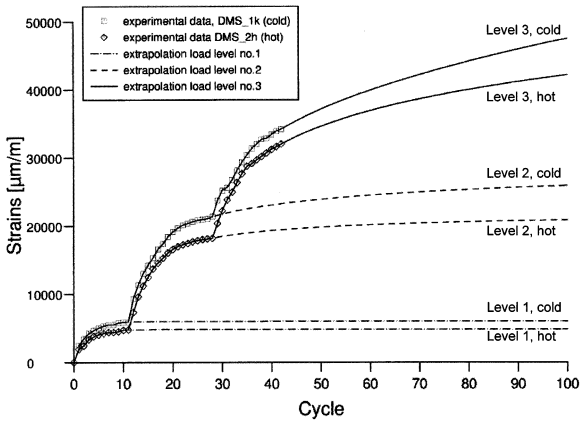

Fig. 3. Measured accumulated strain with extrapolation.

3. Description of test

3.1. Cyclic tensile–compressive tests on material specimens

To determine the load level for the shakedown tests, cyclic tensile–compressive tests were first carried out on material specimens at the representative strain amplitudes for the test load of $\pm 1\%$ at four temperature levels (20°C, 100°C, 200°C, 300°C). Twenty cycles were carried out for each temperature level. The specimen material for the cyclic tensile–compressive tests originated from the same material batch as the material for the bars of the test specimen, and both materials were also subjected to the same heat treatment.

3.2. Load sequence

The chronological load sequence for a load cycle is as follows:

1. mechanical load application (see Fig. 2, bottom);
2. heating of test bars;
3. constant temperature;
4. cooling;
5. mechanical unloading.

The mechanical load to be applied in combination with temperature in the individual load steps was determined in advance such that the values lie within the shakedown range (see Section 4).

3.2.1. Test results

3.2.1.1. Thermal results. The following temperature distributions were measured:

Load step 1: $T_{\max} \approx 200°C$;
Load step 2: $T_{\max} \approx 250°C$;
Load step 3: $T_{\max} \approx 300°C$.

The temperatures measured for load step 1 are shown by way of example in Fig. 2 (top).

3.2.1.2. Strain results. Fig. 3 shows the accumulated strain recorded at the end of each load cycle. The strain history was extrapolated beyond the performed cycles in accordance with Wolters, 1996. Plastic design cannot be based on a stress estimate, as the stresses do not enable separation of the plastic range from the failure range. Plastic design must take account of the characteristic development of plastic strain during structural failure:

- collapse due to unrestricted plastic yield;
- incremental collapse due to accumulation of plastic strain over all cycles (ratcheting);
- Low Cycle Fatigue (LCF) induced by alternating plastification.

In the case of LCF and ratcheting, the plastic strain increments are still present. In the case of elastic deformation, however, the plastic strain values ε^p for the given load become steady-state in nature, i.e. the following applies for $t \to \infty$:

$$\lim \dot{\varepsilon}^p(x,t) = 0$$

for all points x from the structure.

To ensure that failure does not occur, the maximum possible plastic dissipation energy must additionally be limited for all points x from the structure. A simple criterion for elastic shakedown can be derived from the first property Wolters, 1996. Let n be the number of the load cycle, and $\dot{\varepsilon}^p(n)$ the plastic strain increment in

load cycle n at the weakest point of the structure. If shakedown of the structure occurs, the accumulation of plastic strain increments must be limited at this point, i.e. a constant c applies, where:

$$\Sigma_{n=1}^{\infty}\left|\dot{\varepsilon}^{p}(n)\right| \leqslant c.$$

The simplest condition for convergence of this sum as a generalized harmonic series is as follows:

$$\left|\dot{\varepsilon}^{p}(n)\right| < a n^{s} \text{ where } s < -1.$$

This means that in a log–log plot of plastic strain across all load cycles in the case of ratcheting, the exponent must be greater than $s = -1$. The measured plastic strain increments were extrapolated using the least squares method. The results of the three load steps for the cold tube and the hot bars are shown in the table below:

Load step	Strain gauge_1k (cold)	Strain gauge_2h (hot)
1	$s = -3.09$	$s = -2.93$
2	$s = -1.30$	$s = -1.51$
3	$s = -0.64$	$s = -0.88$

It can be concluded from the stated shakedown criterion that load step 1 lies within the shakedown range, while load step 3 lies outside the shakedown range so that ratcheting occurs with the prevailing uniaxial load. Due to the exponents $s = -1.30$ and $s = -1.51$ at the cold tube and at the hot bar, load step 2 is at the limit of the shakedown range. Due to the small number of measured values, it is not possible to decide whether or not shakedown occurs in load step 2.

4. Advance calculation of shakedown loads for the test

Data on the magnitude of the mechanical and thermal loads to be applied were important for performance of the test. A direct procedure for determining shakedown loads, which has been implemented in the PERMAS FEM program INTES Publication, 1988, was used for this purpose Staat and Heitzer, 1999. The shakedown load was determined by solving an optimization problem using the existing FE mesh as for the incremental analysis. The results obtained in this way are shown in the interaction diagram in Fig. 4.

Shakedown or ratcheting occurs as a function of the primary load (application of load by the tensile test machine) and the secondary load (temperature at the test bars). The pressure and temperature loads associated with the three marked points in Fig. 4 were selected for the test. These loads correspond to the maximum values of the three load steps. According to the advance calculation, shakedown should occur in load step 1 ($T = 200°C$, $p = 75$ MPa) and ratcheting in load step 3 ($T = 300°C$, $p = 85$ MPa).

The results calculated in this way were also used to verify this technique through testing.

5. Incremental elasto-plastic analysis

5.1. Analytical model

Due to load and geometrical symmetries, modeling of a 1/12 section is sufficient for the analyses. Fig. 5 shows one-third of the FE model for the test specimen. The analyses were carried out using the ANSYS program [ANSYS, 1997].

5.2. Thermal analyses

Non-steady-state temperature field calculations were used to determine the thermal loads for the structural analyses. The ambient temperatures and heat transfer coefficients were selected such that the measured temperature histories resulted.

5.3. Structural analyses

5.3.1. Load

The load was applied in steps in accordance with Section 3.2. One load cycle comprised a total of 30 load steps. Fig. 6 shows the load history for

the three load levels. The mechanical load was applied as a compressive load in accordance with the force of the tensile test machine. The thermal load was applied for the corresponding time on the basis of the results of the thermal analysis.

5.3.2. Cyclic stress–strain curves

Stress–strain curves for the elasto-plastic analyses were determined for the first seven cycles from the cyclic tensile–compressive tests on material specimens (in accordance with Section 3.1). Almost no further hardening can be observed after the seventh cycle.

5.3.3. Material models for elasto-plastic analyses

The material models currently implemented in ANSYS are compared with other models in Bruhns et al., 1988; Sester et al., 1998. ANSYS implementations for the models of Ohno/Wang and Jiang are published Weiss and Postberg, 1997. The analyses were performed with two different material models:

1. Multilinear kinematic behavior with and without consideration of cyclic hardening in accordance with ANSYS, 1997. This is the overlay model from the Besseling models class already proposed on a one-dimensional basis by Masing. It is assumed that the material consists of elastic-ideal plastic micromodels in parallel, which exhibit different yield stresses given the same Young's modulus.
2. Generalized Frederick and Armstrong model according to Chaboche in the ANSYS implementation in accordance with Weiss and Postberg, 1997.

It contains the Von Mises yield condition F, and the kinematic and isotropic hardening with the current stresses σ and the backstresses α:

$F(\sigma\text{-}\alpha) = k + R$

Kinematic hardening: $\alpha = \Sigma_1^m \alpha_1$, where

$d\alpha_i = C_i d\varepsilon^{pl}\text{-}\gamma_i \alpha_i d\varepsilon_{eq}^{pl}$, $i = 1,...,m$

(in the following: $m = 3$)

Isotropic hardening: $R = \Sigma_1^n R_i$ where

$dR_i = b_i(Q_i\text{-}R_i)d\varepsilon_{eq}^{pl}$, $i = 1,...,n$

(in the following: $n = 1$)

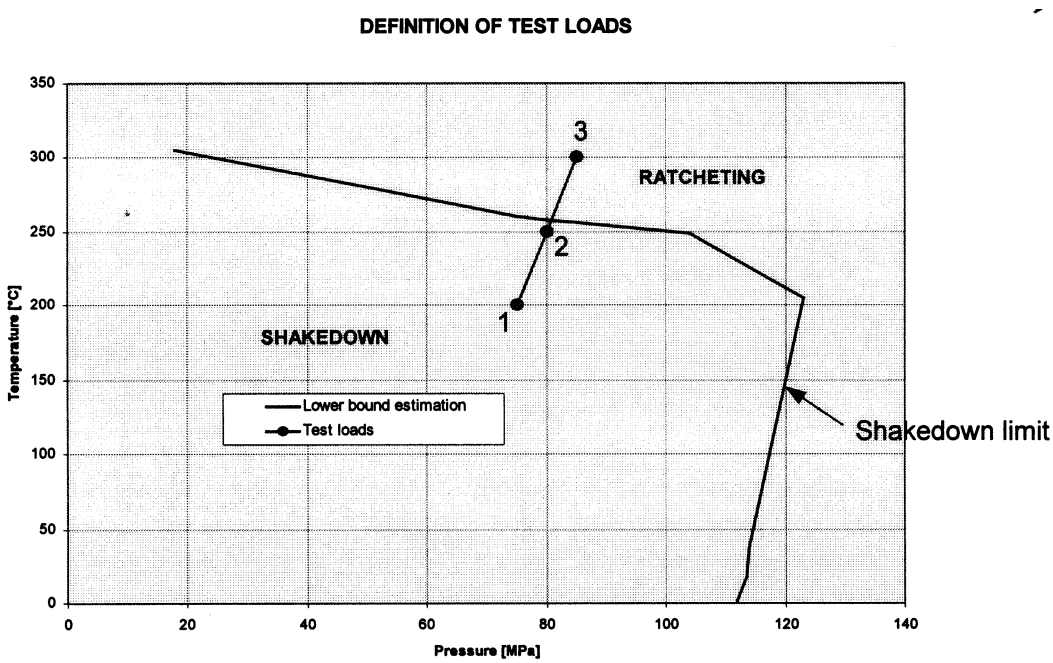

Fig. 4. Interaction diagram as result of shakedown analysis selected test loads at level 1, 2, 3.

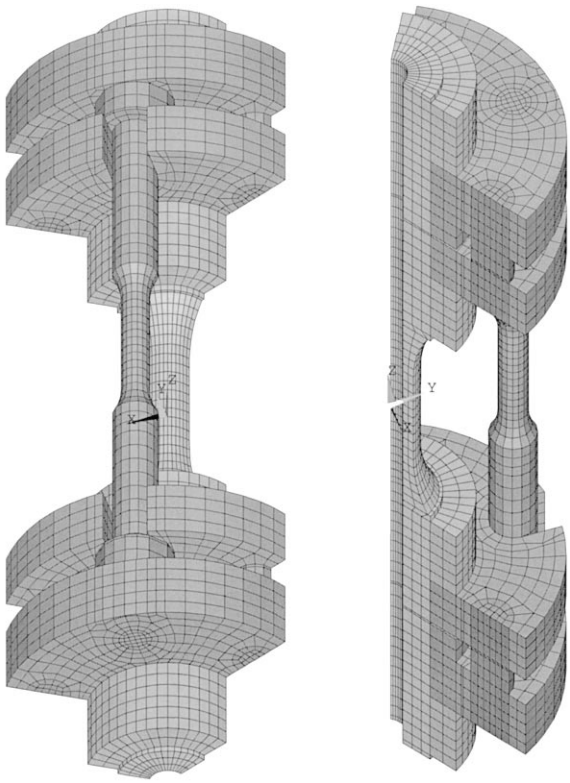

Fig. 5. LISA four bar experiment, finite element model.

The curves used for plastic strain in the Chaboche model were determined using the least squares method from the monotonic stress–strain curves (shown as a progression in Fig. 7) measured in the test, for the temperatures $T = 20°C$, 100°C, 200°C and 300°C. Fig. 8 shows the three parts of the kinematic hardening formula used to make up the stress-strain curve for $T = 20°C$. Fig. 9 compares the hysteresis diagrams from the test with the curves obtained for $T = 20°C$ using the isotropic hardening formula.

5.3.4. Analyses carried out

The following analyses were carried out for load step 1:

a. Besseling model with multilinear kinematic behavior and monotonic stress–strain curves;
b. Besseling model with multilinear kinematic behavior and cyclic stress–strain curves;
c. material model according to Chaboche with kinematic hardening;
d. material model according to Chaboche with kinematic and isotropic hardening.

Due to the findings obtained from these analyses, the following further analyses were carried out for all three load steps:

e. Besseling model with multilinear kinematic behavior and monotonic stress–strain curves;
f. Besseling model with multilinear kinematic behavior and cyclic stress–strain curves;
g. Analyses at increased temperature using the cyclic stress–strain curves.

To take account of possible inaccuracies in temperature measurement and in the thermal analyses, the structural analyses were repeated at higher temperatures. The originally specified temperatures at the outer hot test bars were increased by 5 K.

6. Comparison of test/analytical results

The diagrams below show the overall strain at the end of each load cycle. All diagrams contain the test results.

Fig. 10 shows a comparison of the results with different material models for the first load step:

Curves 5, 6: Besseling model with monotonic stress–strain curves (as per part a) of the previous section).

Curves 7, 8: Chaboche model with kinematic hardening only (as per part c) of the previous section).

Curves 9, 10: Chaboche model with kinematic and isotropic hardening (as per part d) of the previous section).

Curves 1–4: Test results.

Fig. 11 shows the influence of material hardening for the first load step:

Curves 7, 8: Besseling model with monotonic stress–strain curves (as per part a) of the previous section).

Curves 5, 6: Besseling model with cyclic stress–strain curves (as per part d) of the previous section).

Curves 1–4: Test results.

Fig. 12 shows the results for all 3 load steps:

Curves 8, 9: Besseling model with monotonic stress–strain curves (as per part e) of the previous section).
Curves 4, 5: Besseling model with cyclic stress–strain curves (as per part f) of the previous section).
Curves 6, 7: Besseling model with cyclic stress–strain curves at increased temperature (as per part g) of the previous section).12
Curves 1–3: Test results.

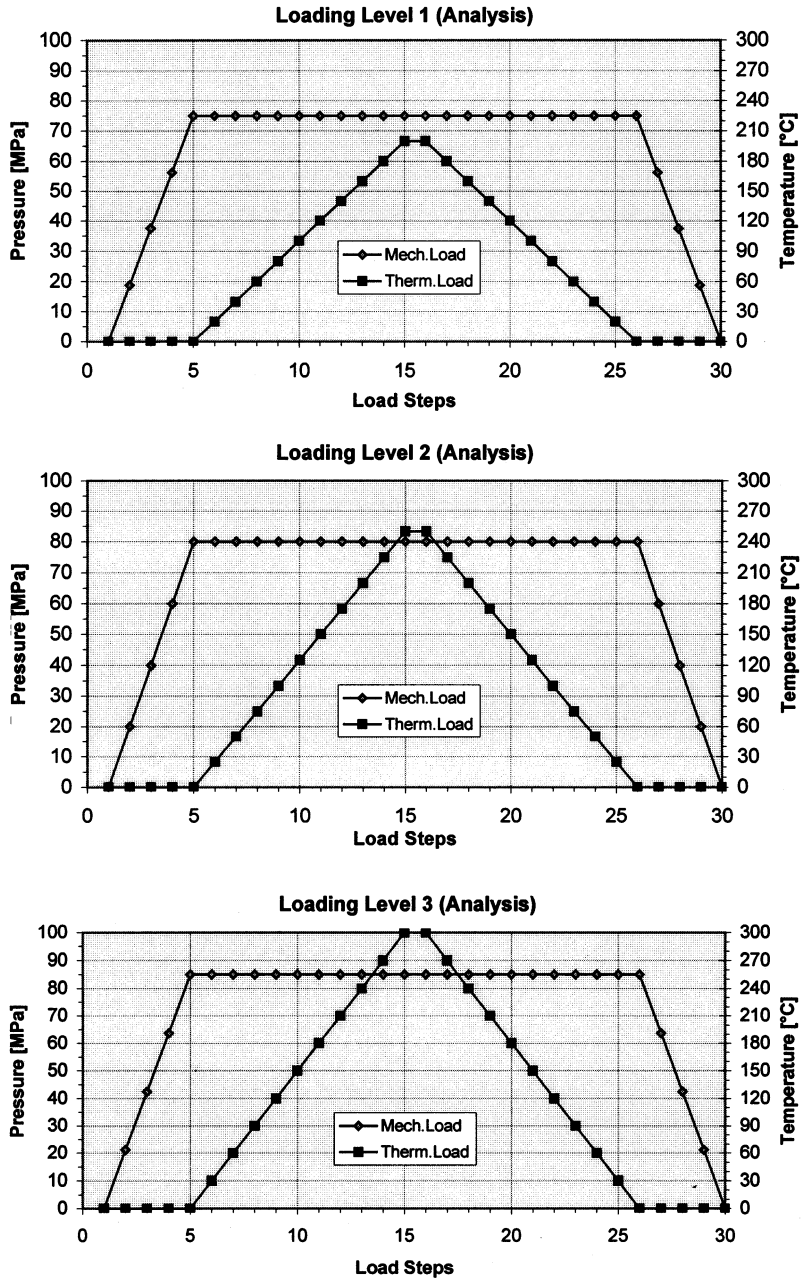

Fig. 6. Load steps for load cycle at level 1, 2, 3.

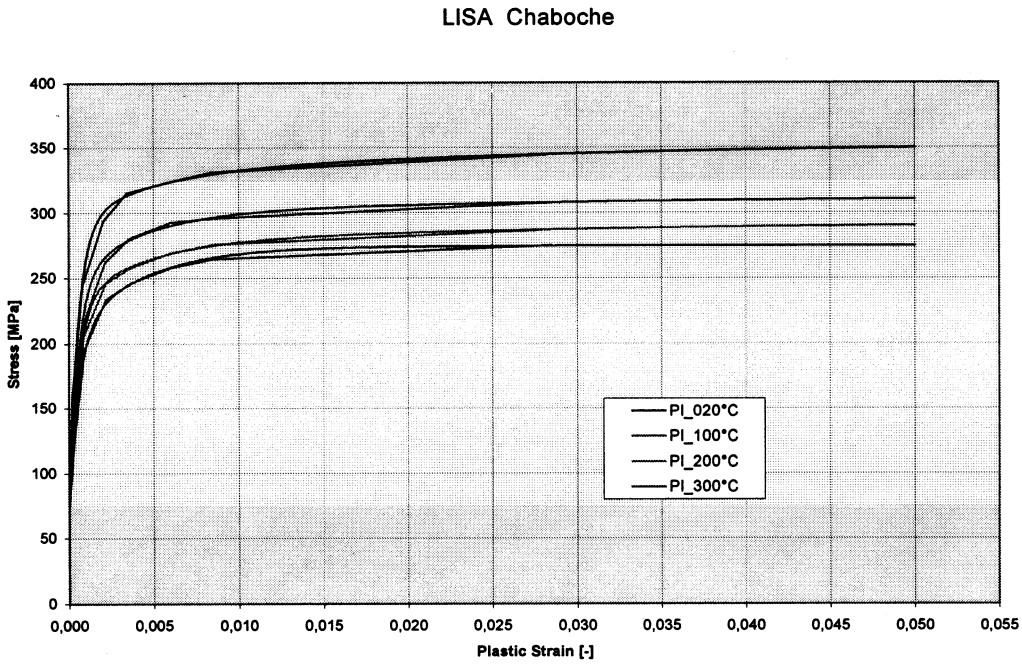

Fig. 7. Stress–strain curves in chaboche model.

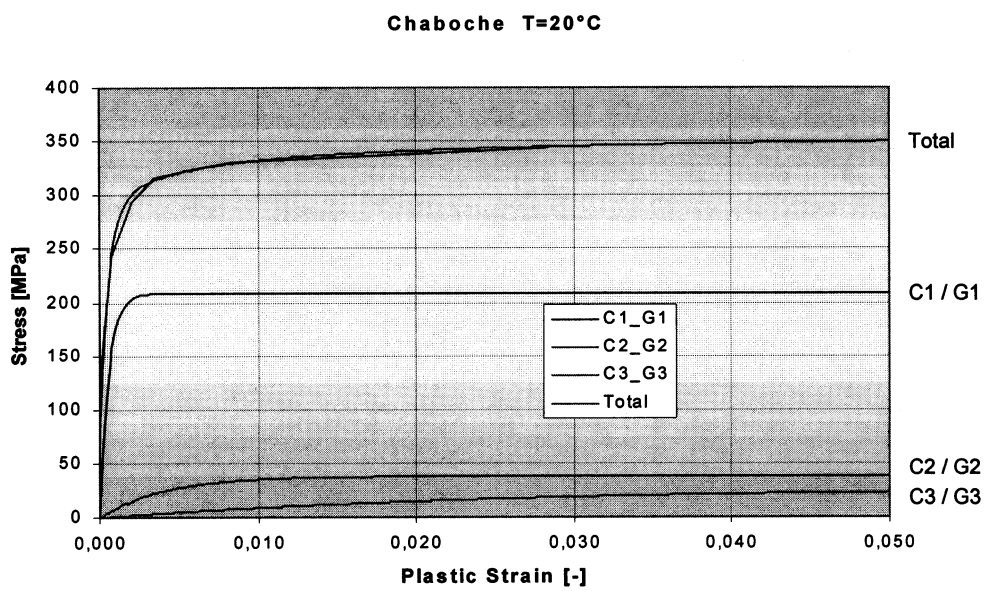

Fig. 8. Combination of 3 components of kinematic hardening approach in Chaboche model.

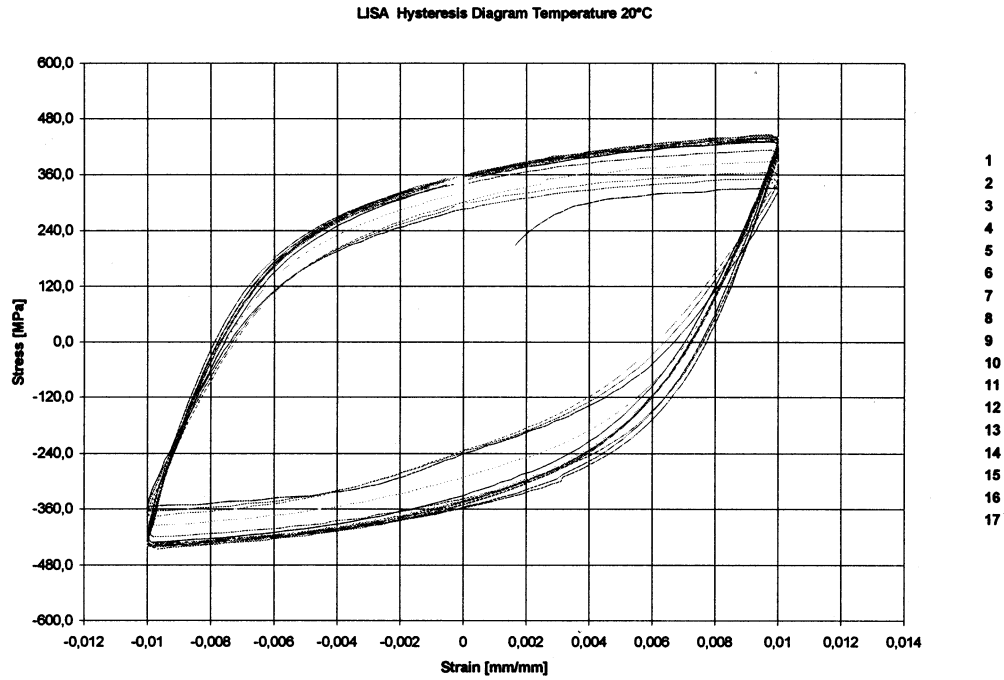

Measured Hysteresis of Material Specimen at 20°C

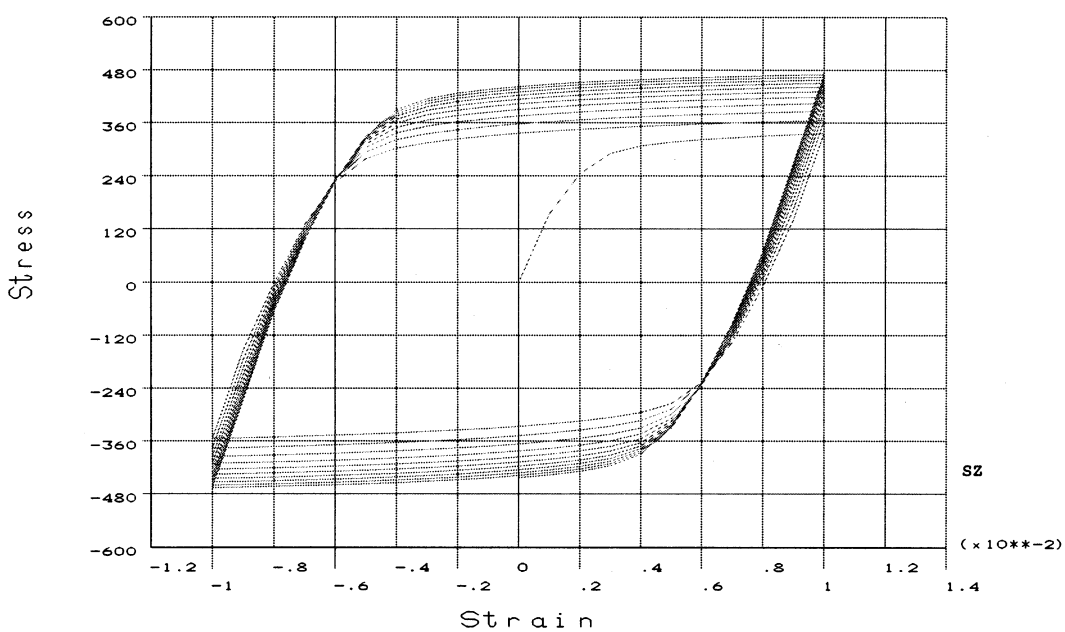

Hysteresis Diagram from Isotropic Hardening Approach in Chaboche Model

Fig. 9. Measured hysteresis of material specimen at 20°C hysteresis diagram from isotropic hardening approach in Chaboche model.

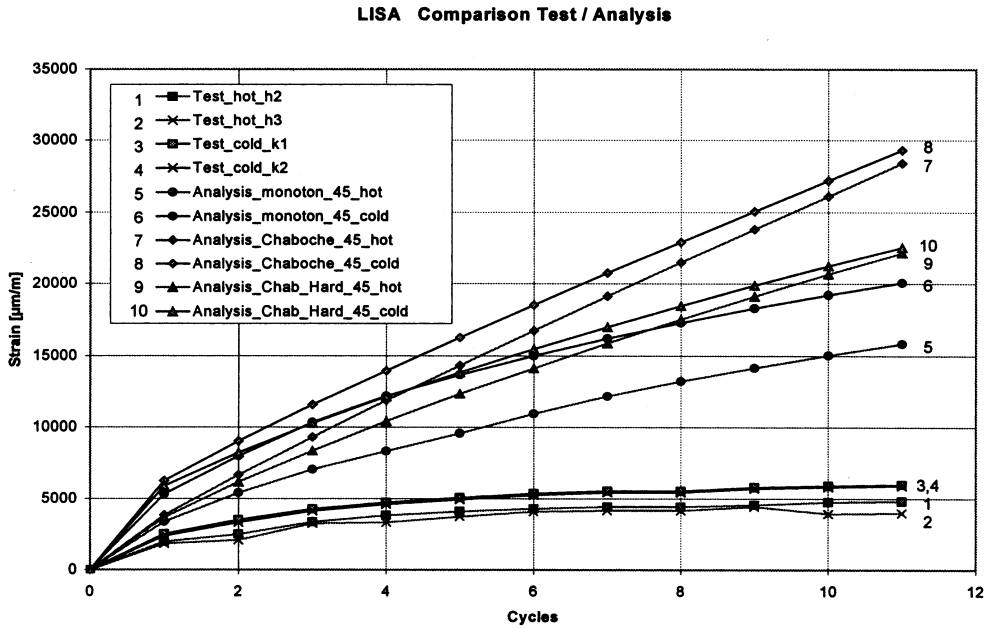

Fig. 10. Comparison test/Analysis load level 1.

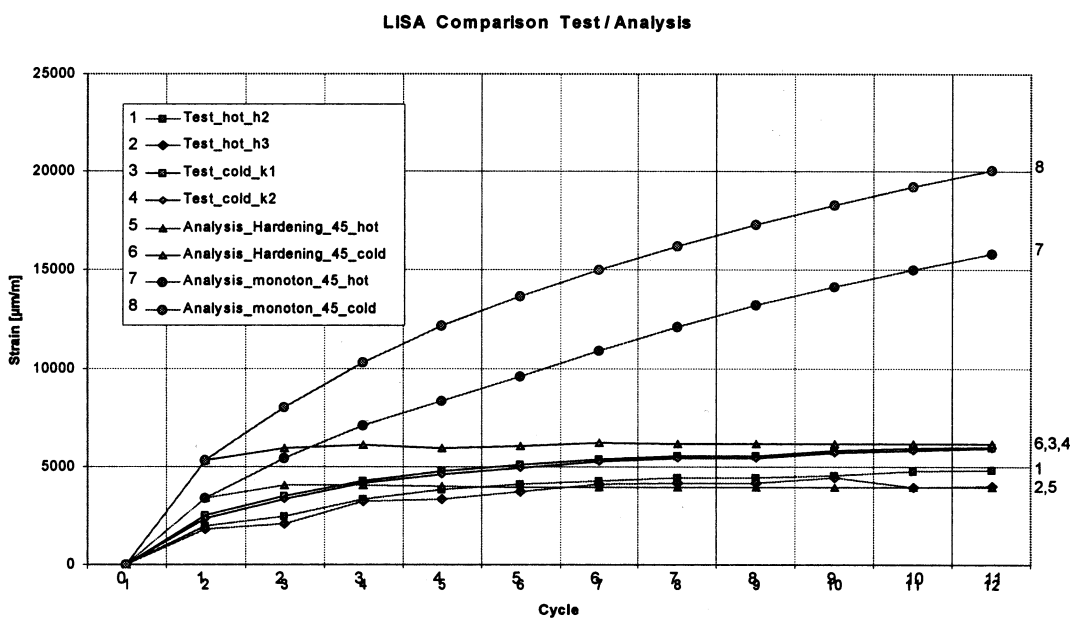

Fig. 11. Comparison test/Analysis load level 1.

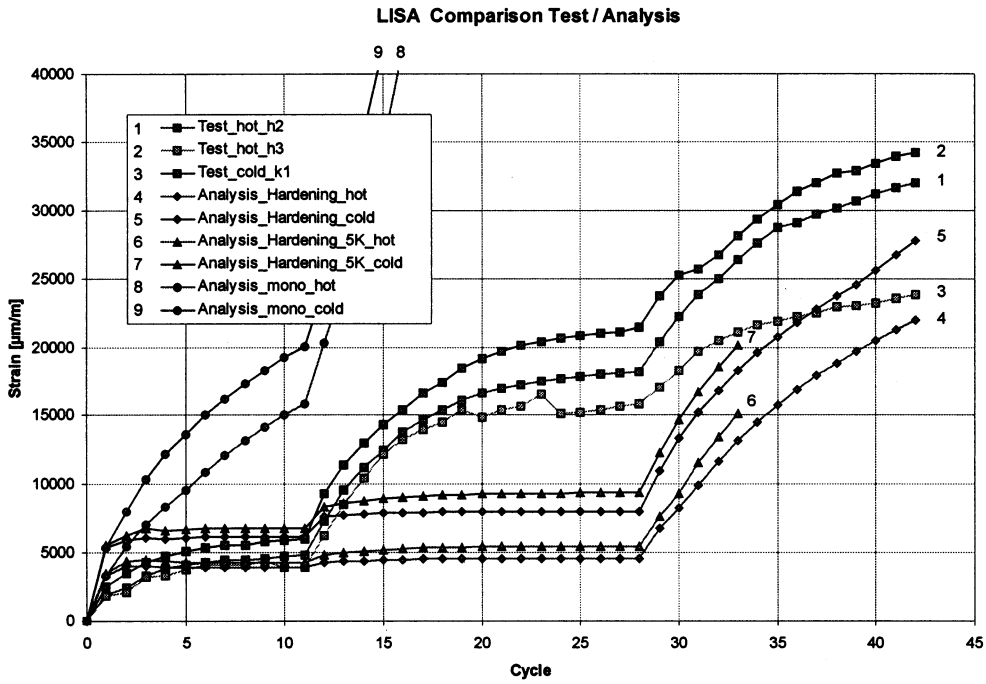

Fig. 12. Comparison test/Analysis load levels 1–3.

7. Conclusions

The tests showed elastic shakedown behavior after the first load step. The second load step was at the shakedown limit. Ratcheting occurred in the third load step.

The results calculated in advance using the shakedown analysis method were confirmed by the tests.

The results from the incremental elasto-plastic analyses enable the following conclusions to be drawn:

- The analyses using the Besseling model with monotonic stress–strain curves showed ratcheting behavior as early as after the first load step. They are thus on the conservative side with respect to the calculated strains.
- The analyses using the Besseling model with the cyclic stress–strain curves resulted in elastic shakedown behavior in the first and second load step, and ratcheting in the third load step.
- The use of the material model according to Chaboche resulted in ratcheting behavior in the first load step, with both kinematic hardening only and with kinematic and isotropic hardening.

Acknowledgements

This work was supported by the European Commission via the Brite-EuRam III program, Project BE 97-4547, Contract BRPR-CT97-0595.

References

ANSYS. Engineering Analysis System, Rev. 5.4, Houston, Pennsylvania, 1997.

Bruhns, O.T. White, P.S., Chaboche, J.L., Eikhoff, J.V.D., 1988. Constitutive modelling in the range of inelastic deformations. CEC Report EN, Brussels.

INTES Publication, 1988. PERMAS User's Reference Manuals No. 202, 207, 208, 302, 404, 405, Stuttgart.

KTA 3201.2, Komponenten des Primärkreises von Leichtwassereaktoren Teil 2: Auslegung, Konstruktion und Berechnung Fassung 6/96.

Ng, H.W., Moreton, D.N., 1982. The Bree-Diagram —

origins and literature — some recent advances concerning experimental verification and strain-hardening materials. In: Wilshire, B. (Ed.), Recent Advances in Creep and Fracture of Engineering Materials and Structures. Pineridge Press, 185–230.

Ponter, A.R.S., 1983. Shakedown and ratchetting below the creep range. CEC Report EUR8702 EN, Brussels.

Sester, M., Mohrmann, R. Böschen, R., 1998. Ratcheting of an austenitic steel under multiaxial and thermomechanical loading: experiments and modeling. In: Rie, K.T., Portella, P.D. (Eds.), Low Cycle Fatigue and Elasto-Plastic Behaviour of Materials, Elsevier, Amsterdam.

Staat, M. Heitzer, M., 1999. LISA, ein europäisches Projekt zur FEM-basierten Traglast-und Einspielanalyse 25. MPA-Seminar, October 6–7, Nuclear Engineering and Design 206, 233–245.

Weiss, E., Postberg, B., 1997. Modellierung von Ratchetting-Effekten bezogen auf Komponenten der Chemie-und Kraftwerkstechnik. 15. CAD.-FEM Users' Meeting, Fulda, 15–17 October.

Wolters, J., 1986. Untersuchungen zum Ratchetting von Segmenten der 'Ersten Wand' zukünftiger Fusionsreaktoren unter zyklischer thermischer und mechanischer Belastung. RWTH Aachen, Dissertation.